SAND2011-0955C

Low-Energy Proton Testing Using Cyclotron Sources

Jonathan A. Pellish, Paul W. Marshall, Carlos M. Castaneda, Robert A. Weller, David F. Heidel, Kenneth P. Rodbell, Kenneth A. LaBel, Melanie D. Berg, Hak S. Kim, Mark R. Friendlich, Anthony M. Phan, Christopher E. Perez, Christina M. Seidleck, James R. Schwank, Marcus H. Mendenhall, and Robert A. Reed

Abstract

We present a set of techniques for low-energy proton testing and analysis, including an assessment of the Crocker Nuclear Laboratory beam line. We stress the importance of in-situ calorimetry and radiation transport simulations.

Corresponding and Presenting Author

- Jonathan A. Pellish is with the NASA Goddard Space Flight Center, Code 561.4, 8800 Greenbelt RD, Greenbelt, MD 20771 USA.
  - Phone: 301.286.6523, Fax: 301.286.4699, Email: jonathan.a.pellish@nasa.gov.

Contributing Authors

- P. W. Marshall is a NASA consultant, Brookneal, VA 24528 USA.
- C. M. Castaneda is with the Crocker Nuclear Laboratory (UC Davis), Davis, CA 95616 USA.
- R. A. Weller, M. H. Mendenhall, and R. A. Reed are with the Department of Electrical Engineering and Computer Science, Vanderbilt University, Nashville, TN 37235 USA.
- D. F. Heidel and K. P. Rodbell are with the IBM T. J. Watson Research Center, Yorktown Heights, NY 10598 USA.
- K. A. LaBel is with the NASA Goddard Space Flight Center, Code 561.4, 8800 Greenbelt RD, Greenbelt, MD 20771 USA.
- M. D. Berg, H. S. Kim, M. R. Friendlich, A. M. Phan, C. E. Perez, and C. M. Seidleck are with MEI Technologies (NASA/GSFC), Lanham, MD 20706 USA.
- J. R. Schwank is with Sandia National Laboratories, Albuquerque, NM 87185 USA.

Session Preference: Dosimetry
Presentation Format: Oral

The authors wish to thank the staff at the UC Davis Crocker Nuclear Laboratory for their dedication to bringing up the new beam line capabilities for low-energy protons, making this work possible. Thanks are also due to Brian Sierawski for helping shake off the Python rust.

This work was supported in part by the NASA Electronic Parts and Packaging program and the Defense Threat Reduction Agency Radiation Hardened Microelectronics program under IACROs #10-4977I and #11-4395I to the NASA. The portion of the work performed at Sandia National Laboratories was supported in part by the Defense Threat Reduction Agency under IACRO #10-4962I, the U. S. Department of Energy, and the NASA Electronic and Parts Packaging program. Sandia is a multi-program laboratory operated by Sandia Corporation, a Lockheed Martin Company, for the United States Department of Energy's National Nuclear Security Administration under Contract DE-AC04-94AL85000.

I. INTRODUCTION

Protons with less than 2 to 3 MeV of kinetic energy, so called "low-energy protons," have been of significant interest to the radiation effects community for the past several years, particularly concerning scaled complementary metal oxide semiconductor (CMOS) designs [1-6]. When Rodbell *et al.* showed that low-energy protons could upset the logic state of 65-nm silicon-on-insulator (SOI) CMOS latches and memory cells [1], possible implications for deleterious on-orbit effects were clear given the abundance of trapped and solar protons in the space environment [4, 7]. Since that point, low-energy proton soft errors have also been reported in 90-nm bulk CMOS [5, 6] and 45-nm SOI CMOS [3].

However, while the soft errors themselves have been covered in detail, little attention has been paid to how the low-energy proton experimental data are gathered – the different particle sources available, operating in-air versus in-vacuum, and the inherent systematic errors associated with measurements based on ion stopping power and range close to the Bragg peak. This work aims to highlight these issues through examples of new proton data on 45 and 32-nm SOI CMOS components in addition to GEANT4 radiation transport simulations using the Vanderbilt Monte Carlo Radiative Energy Deposition (MRED) code [8]. We do this, not to call into question previous results, but to present relevant issues and lay out ground rules for hardness assurance rate calculations. This is necessary, since scientific and engineering investigations on this topic are likely to progress.

II. PROTON FACILITY AND DATA COLLECTION

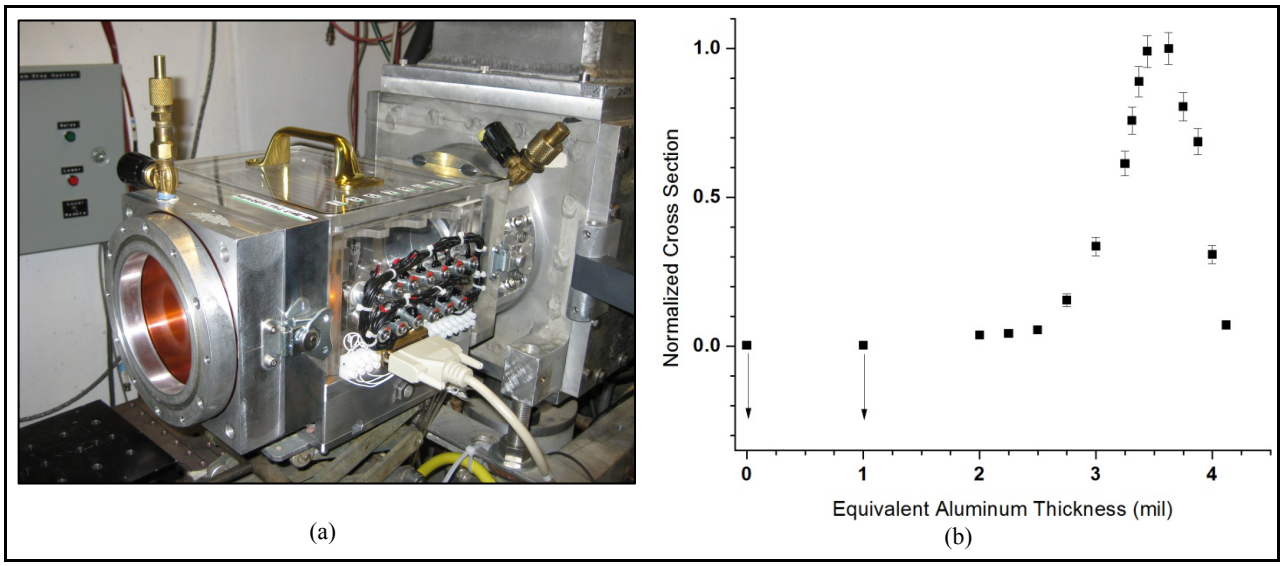

Figure 1: (a) New beam degrader system at the CNL, shown here when it is bolted onto the end of the Radiation Effects Facility beam line in the north cave. Through a combination of permanent and induced magnets, up to thirteen rings with aluminum or polyethylene terephthalate (Mylar) foils can be moved into and out of the path of the beam from the users' station in the south cave. The box with the rings is under the same vacuum as the beam line. (b) Low-energy proton data (degraded 6.5-MeV tune in-air) on an unhardened 45-nm SOI CMOS latch chain. The downward arrows indicate limiting cross sections. These data were taken at a 70° tilt angle, increasing both the effective stopping power of the protons and the window of opportunity for upset.

We used the Crocker Nuclear Laboratory (CNL) at the University of California/Davis as the primary low-energy proton testing facility for this work [9]. The CNL uses a 76-in cyclotron to accelerate protons up to a maximum of 68 MeV with fluxes from a few tens of protons/(cm^2·s) up to more than 10^{11} protons/(cm^2·s). While it would be possible to degrade a 60 MeV beam to a few MeV, the energy straggle in the beam would be unacceptable. Sierawski *et al.* presented an example of this in Section VI their 2009 paper [4]. For in-air irradiations, the CNL accelerates H_2^+ to 13 MeV, which breaks into two protons as soon as it hits the upstream

Table I: Basic setup for the CNL beam line with no user-applied degraders. If aluminum and/or Mylar degraders are employed, they would go in between the third Al SEEM foil and the kapton exit window. This location is inside the acrylic box shown in Figure 1. The positions are such that the surface of the detector is at z = 0 cm. Everything before the kapton foil is separated by vacuum.

Beam Line Element	Thickness (mm)	*Z*-Position (mm)
Tantalum scattering foil	0.00635	-4252.549225
Aluminum SEEM foil (1 of 3)	0.00635	-370.142875
Aluminum SEEM foil (2 of 3)	0.00635	-350.136525
Aluminum SEEM foil (3 of 3)	0.00635	-330.130175
Kapton exit window	0.127	-30.0635
Air gap	30.	-15.
Silicon surface barrier detector	0.3	0.15

tantalum scattering foil – each proton has half the total kinetic energy, or 6.5 MeV. Table I shows the basic beam line setup with no degraders. While the air gap can change depending on the test configuration, the other materials cannot be reduced. This setup has been used for gathering data published in a number of previous papers [2-4].

Since most scaled microelectronics are insensitive to proton direct ionization at incident energies above 2 MeV, a majority of the protons have to come to rest very close to the sensitive volume so that their stopping power will deposit sufficient energy and cause a soft error. This window of opportunity for upset is larger for bulk CMOS than for SOI CMOS technologies. The window size is also affected by energy straggling and angular dispersion present in the proton beam [10]. Energy straggling is proportional to the amount of mass in the beam path and the difference between the tuned and incident proton energies. Figure 1(b) shows an example of a 45-nm SOI CMOS latch chain tilted to angle to increase the size of the window of opportunity. Much of the low-energy proton data presented to date has been taken at normal incidence, but angular sensitivity is important to understand. With the device under test tilted, more protons are able to upset the latch stages, effectively increasing the window of opportunity relative to normal incidence.

The size of this window affects the energy-width of the low-energy proton cross section. Taken out of context, this is just a systematic effect. However, current on-orbit rate calculations approach these data by integrating under the low-energy portion of the curve [2, 5]. The radiation effects community has not presented a suitable method to account for angled irradiations, instead relying on normal incident irradiations. Accurate testing and subsequent interpretation must be able to account for the additional energy width imparted by beam line and setup effects. We will discuss this further in the final paper.

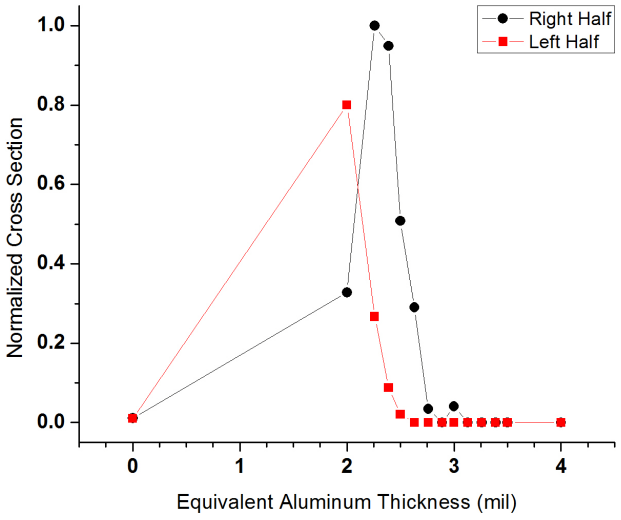

Figure 2: 45 nm SOI SRAM low-energy proton data (degraded 6.5-MeV tune in-air) showing the normalized cross section of bits on the left-hand-side and the right-hand-side of the SRAM die. Error bars are smaller than the data points.

The energy-width dependence of the cross section increase at low energy is further complicated when the device under test adds mass to the beam path – as is the case for controlled collapse chip connection (flip-chip) devices. In this case, the substrate of the device is usually thinned to avoid increasing beam energy straggle. An example of where this may matter is shown in Figure 2 with low-energy proton data gathered on a 45-nm SOI CMOS static random access memory (SRAM) – original data set published in [3]. This flip-chip device was thinned to approximately 100 μm prior to irradiation. The device has six organizational sextants, each split into a right- and left-half. It is evident from these data that the substrate thickness is not entirely uniform – the left-half is thicker than the right-half – though x-ray inspection revealed the difference was likely less than 15 μm from one side to the other. Since the protons are stopping close to the silicon layer, this small difference can have a large impact. The final paper will discuss data collection impacts on 45 and 32-nm SOI CMOS latches in more detail.

III. Proton Transport Simulations

Several years ago, when we started working with low-energy protons at the CNL, we used the Stopping and Range of Ions in Matter (SRIM) program [11, 12] to compute the mean energy of protons incident on the surface of the device under test. However, this approach yielded differences with measured data, particularly when proton kinetic energies dropped below 2 MeV. We made the decision to implement MRED for kinetic energy and calorimetric calculations by building up a model of the CNL beam line. Figure 3(a) shows a comparison of MRED and SRIM to an Ortec B-18-150-300 fully depleted silicon surface barrier detector (SBD) for a given beam line and degrader configuration; MRED shows good agreement. We tested several of these scenarios to see if we could isolate the difference between MRED and SRIM – *i.e.*, using a planar target stack in MRED (like SRIM). We attribute the difference to electromagnetic transport and the virtual detector configuration, not the organization or the composition of layers, topics we will discuss thoroughly in the final paper.

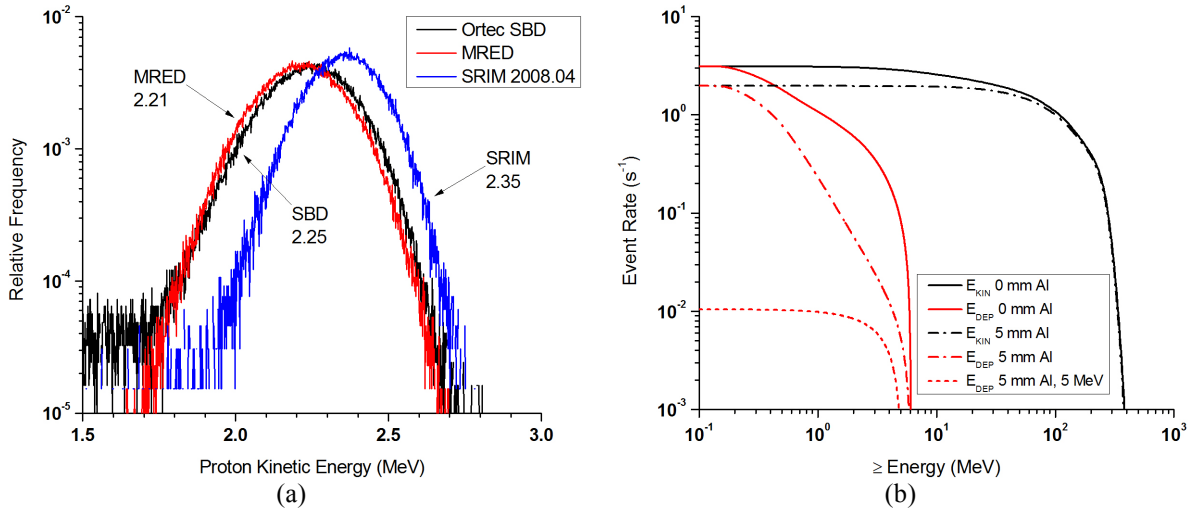

Figure 3: (a) Comparison of MRED and SRIM simulations to an Ortec SBD for the standard CNL beam line given in Table I, though with a 110-mm air gap plus 0.0508 mm of aluminum and 0.0127 mm of Mylar degrader. The values below the text labels are the mean energies of the distributions in MeV. The distributions represent approximately 125k events in all cases. (b) Event rates on the virtual SBD for transported unidirectional trapped proton spectrum energy deposition and kinetic energy on-target for three different cases: 1) CNL beam line with 110-mm air gap, 2) CNL beam line with 110-mm air gap and 5 mm of aluminum degrader, 3) same as 2) though with the maximum proton kinetic energy on-target limited to 5 MeV. Note that low-energy protons on-target are a small component of the overall transported spectrum.

Beyond scientific and engineering research conducted previously, we would like to understand how low-energy protons may impact devices and systems on-orbit, since all spacecraft trajectories must account for either trapped or solar proton environments. Protons reaching devices within spacecraft must penetrate shielding, modifying the incident spectrum and reducing the number of protons with less than 2 MeV of kinetic energy – these are protons from a sliver of the incident differential spectrum. Traditionally, we use radiation transport codes like NOVICE [7, 13] and FASTRAD [14] to transport omnidirectional protons through spacecraft shielding to calculate emerging fluence, flux, or pulse height spectra. Figure 3(b) shows this same kind of proton transport using MRED. However, in this case, we use a unidirectional flux of trapped protons from a circular low-earth polar orbit and the "shield" is the CNL beam line. The result is an event rate on the target, a SBD in this case, but it could be any type of electronic component as well. We intend to use simulations like this to gain the ability to design specific low-energy proton experiments that more accurately represent the on-orbit environment for different trajectories and shielding configurations. There are two approaches to be evaluated for empirical on-orbit rate calculations using accelerated data: 1) use a series of specific quasi-monoenergetic cross sections (in air or vacuum) to approximate the transported on-orbit proton spectrum, and 2) use a degraded high-energy spectrum in vacuum, which is similar to the way that accelerated

neutron testing is conducted. Approaches like these could provide a means to compute on-orbit rates, validated with ground test data, which implements MRED in a proven configuration [4, 8, 15].

IV. Discussion and Summary

The idea of using low-energy protons on scaled or commercial hardware has been around for at least five years [16]. However, only in the past few years has the idea of proton direct ionization soft errors become widely accepted. While using a Van de Graaff accelerator certainly has advantages over a cyclotron accelerator source for energy precision, routine beam testing for qualification purposes often defaults to the use of cyclotron proton sources because of the larger energy range and because it is also financially advantageous to do all testing at a single facility. This work discusses some of the most relevant challenges when using cyclotrons for low-energy proton testing and how the data might be leveraged.

We have outlined an approach to accurately simulate a realistic cyclotron beam line using an advanced Monte Carlo toolset. We used this simulation framework to study the effect of a low-energy proton beam on a silicon target. We also presented the idea of transporting space environment protons down ground-based beam lines. Utilization of these methods will enable insight to the on-orbit environment and how we might approximate it with a ground test facility. Comparing transmitted trapped and solar proton energy spectra to the low-energy, quasi-monoenergetic version will provide the necessary information to best direct low-energy accelerated tests.

V. References

[1] K. P. Rodbell, *et al.*, "Low-Energy Proton-Induced Single-Event-Upsets in 65 nm node, Silicon-on-Insulator, Latches and Memory Cells," vol. 54, no. 6, pp. 2474-2479, Dec. 2007.

[2] D. F. Heidel, *et al.*, "Low energy proton single-event upset test results on 65 nm SOI SRAM," *IEEE Trans. Nucl. Sci.,* vol. 55, no. 6, pp. 3394-3400, Dec. 2008.

[3] D. F. Heidel, *et al.*, "Single-event upsets and multiple-bit upsets on a 45 nm SOI SRAM," *IEEE Trans. Nucl. Sci.,* vol. 56, no. 6, pp. 3499-3504, Dec. 2009.

[4] B. D. Sierawski, *et al.*, "Impact of low-energy proton induced upsets on test methods and rate predictions," *IEEE Trans. Nucl. Sci.,* vol. 56, no. 6, pp. 3085-3092, Dec. 2009.

[5] E. H. Cannon, *et al.*, "Heavy Ion, High-Energy, and Low-Energy Proton SEE Sensitivity of 90-nm RHBD SRAMs," *IEEE Trans. Nucl. Sci.,* vol. 57, no. 6, pp. 3493-3499, Dec. 2010.

[6] N. Haddad, *et al.*, "Heavy ion, high energy and low energy proton SEE sensitivity of 90-nm RHBD SRAMs," presented at the European Conf. on Radiation and Its Effects on Components and Systems, Langenfeld, Austria, 2010.

[7] J. A. Pellish, *et al.*, "Impact of Spacecraft Shielding on Direct Ionization Soft Error Rates for Sub-130 nm Technologies," *IEEE Trans. Nucl. Sci.,* vol. 57, no. 6, pp. 3183-3189, Dec. 2010.

[8] R. A. Weller, *et al.*, "Monte Carlo Simulation of Single Event Effects," *IEEE Trans. Nucl. Sci.,* vol. 57, no. 4, pp. 1726-1746, Aug. 2010.

[9] C. M. Castaneda, "Crocker Nuclear Laboratory (CNL) radiation effects measurement and test facility," in *IEEE Radiation Effects Data Workshop*, Vancouver, BC Canada, 2001, pp. 77-81.

[10] "Stopping Powers and Ranges for Protons and Alpha Particles," International Commission on Radiation Units and Measurements Report 49, May 1993.

[11] J. F. Zeigler, "SRIM-2003," *Nucl. Instr. and Meth. B,* vol. 219-220, pp. 1027-1036, Jun. 2004.

[12] J. F. Zeigler and J. P. Biersack. (2010). *Stopping and Range of Ions in Matter*. Available: http://www.srim.org/

[13] T. M. Jordan, "An adjoint charged particle transport method," *IEEE Trans. Nucl. Sci.,* vol. 23, no. 6, pp. 1857-1861, Dec. 1976.

[14] T. Beutier, *et al.*, "FASTRAD: new tool for radiation prediction," in *European Conf. on Radiation and Its Effects on Components and Systems*, Noordwijk, The Netherlands, 2003, pp. 181-183.

[15] K. M. Warren, *et al.*, "Monte-Carlo based on-orbit single event upset rate prediction for a radiation hardened by design latch," *IEEE Trans. Nucl. Sci.,* vol. 54, no. 6, pp. 2419-2425, Dec. 2007.

[16] S. Gerardin, *et al.*, "Exploiting a low-energy accelerator to test commercial electronics with low-LET proton beams," presented at the European Conf. on Radiation and Its Effects on Components and Systems, *IEEE*: Athens, Greece, 2006.